

TEMPERATURE INVESTIGATION IN REAL HOT RUNNER SYSTEM USING A TRUE 3D NUMERICAL METHOD

Tzu-Chau Chen¹, Yan-Chen Chiu¹, Marvin Wang¹, Chao-Tsai Huang¹, Cheng-Li Hsu², Chen-Yang Lin², Lung-Wen Kao²

- 1. CoreTech System (Moldex3D) Co., Ltd., ChuPei City, Hsinchu, Taiwan*
- 2. ANNTONG Co., Ltd., Sanchong, New Taipei City, Taiwan*

Abstract

Hot runner technology has been the solutions to the molding problems on many plastic injection products, such as automobile bumper, LCD/TV cover, bottle cap and so on. However, the mechanism behind the hot runner system is too complicated to be fully understood. In addition, there exist some critical issues in the current hot runner technology, such as temperature control issues, flow imbalance, and material degradation. As a result, the simulation technology is highly needed for hot runner designers and makers to examine their designs before the real manufacturing. Through simulation analyses, designers and manufacturers are able to catch the potential issues on their hot runner systems and revise their designs. Hot runner simulation technology helps with the investigations into the behavior in hot runner system. In this paper, a true 3D numerical method is proposed and applied to investigate the temperature behavior in a real hot runner system for PC material. The experiment is conducted and the simulating result is compared with that from the experiment for the validation purpose.

Introduction

Runner system plays a very important role in injection molding process [1-4]. The purpose of runners is to transport melt from injection machine nozzle to the cavities. Runner designs have a great influence on the qualities of molded parts. The quality runner design is very helpful in improving product qualities. However, traditional cold runner systems have certain inherent issues, such as material waste, regrind problem, increased molding cycle and so on. Moreover, poor product cosmetics, such as welding line and low gloss matter, are commonly seen with the use of traditional cold runner. As a result, hot runner technology [5-10] has become the trend in order to deal with these issues in injection molding process. Hot runner technology can provide the benefits of reduced injection pressure/clamping force required, easy cavity filling, decreased cycle time,

improved product quality, and energy/material saving. For hot runner applications, it has been applied to many large-sized plastic parts, such as bumper, automobile dashboard, TV/LCD front/back cover etc. Hot runner technology is also used for some common plastic products: bottle caps, food plastic containers and so on.

A hot runner system is mainly composed of hot runner gate, hot nozzle, manifold and heating coil. There are various types of designs for each component. For example, hot runner gate options are very diverse, including hot-tip gate, thermal sprue gate, edge gate, and valve gate. The combinations of different component designs affect the hot runner system performance. The dimension of each component is also very influential to its behavior. Hence, the mechanism in the hot runner system is so complicated that it is difficult to be fully understood. In addition, there exist some critical issues in the current hot runner technology, such as temperature control issues, flow imbalance, and material degradation. As a result, a simulation technology is highly required for hot runner designers and makers to examine their designs before the real production. Through simulation analysis results, designers and manufacturers are able to investigate temperature profile, pressure drop, shear heating effect etc. and find the potential issues on their hot runner systems. Hot runner simulation technology is very useful in understanding complex hot runner system. Therefore, it can help improve hot runner system designs and product qualities.

In this paper, a true 3D numerical method is proposed to simulate the behavior of a real hot runner system for PC material. The CAE model can be constructed without too much effort by importing each major hot runner components, defining their attributes, meshing automatically. The boundary conditions, heat conduction faces, can be also properly defined to match with the experiment. The dynamic melt temperature profile in the hot runner system can be simulated and investigated. The real hot runner experiment is conducted and the temperature is measured at the locations of interest. The simulating results are compared with those from the experiment to validate this simulation technology. The

preliminary result indicates good agreement both in trend and magnitude.

Numerical Simulation

A true 3D numerical method is developed and used to simulate the behavior of hot runner systems. The CAE model can be created without too much effort by using Moldex3D. Each major hot runner component is imported, attribute-defined, and meshed automatically in the preprocessing stage. Also, the boundary conditions can be defined to match with the experiment in a convenient way. The defined BC surfaces are assumed direct contact with the metal mold. The heat escapes from these areas due to heat conduction. On the other hand, the undefined surfaces are assumed contact with air. Those areas do not have contributions to heat loss in the simulation analysis. Heating coils can be imported in .stl format to match with the real geometry in the experiment. In the simulation, heating coils can be controlled by two heating methods: by temperature or by power. For “by temperature”, the heating coils are given a specific temperature (°C) and maintain this value all the time in the analysis. For “by power” method, the heating coils are given a power value (W or W/cm²) and controlled by “on/off” method. Each heating coil is assigned a sensor node. This sensor node detects the temperature and determines whether the corresponded heating coil is switched on or off. The target temperature and range need to be defined for the analysis.

A three-dimensional, cyclic, transient heat conduction problem with boundary conditions on hot runner component surfaces is involved. The overall heat transfer phenomenon is governed by a three-dimensional Poisson equation [11-15].

$$\rho C_p \frac{\partial T}{\partial t} = k \left(\frac{\partial^2 T}{\partial x^2} + \frac{\partial^2 T}{\partial y^2} + \frac{\partial^2 T}{\partial z^2} \right) \quad (1)$$

where T is the temperature, t is the time, x , y , and z are the Cartesian coordinates, ρ is the density, C_p is the specific heat, k is the thermal conductivity. The equation holds for both hot runner components and part component except with different thermal properties. The initial mold temperature is assumed to be equal to the input of initial settings. The initial part temperature distribution is obtained from the analysis results at the end of filling and packing stages.

$$T(0, \vec{r}) = \begin{cases} T_c, & \text{for } \vec{r} \in \Omega_m \\ T_p(\vec{r}), & \text{for } \vec{r} \in \Omega_p \end{cases} \quad (2)$$

In this study, the effect of thermal radiation is ignored. The conditions defined over the boundary surfaces and interfaces of the mold are specified as,

$$\text{for } t \geq 0, \quad -k_m \frac{\partial T}{\partial n} = h(T - T_o) \quad (3)$$

Where n is the normal direction of mold boundary, h is heat transfer coefficient. On the exterior surfaces of the moldbase,

$$h = h_{air}, T_0 = T_{air} \quad \text{for } \vec{r} \in \Gamma_m \quad (4)$$

Description of CAE Model

In this study, this numerical simulation technology is applied to a real hot runner system manufactured by ANNTONG IND. CO. LTD. This system includes the part, hot runner nozzle, 3 sets of heating coils, 3 brass bushings which the heating coils are wrapped around, a metal mold, and other bushing components. The dimension of the entire moldbase is 250.00 x 250.00 x 320.00 mm. The material for the metal mold is P20. The thermoplastic material for the melt is PC (Panlite L-1225Y). The constructed CAE model for this hot runner system is shown in Figure 1. The figure 1 also indicates the materials used for each hot runner component. The component shown in the same color is made of the same material.

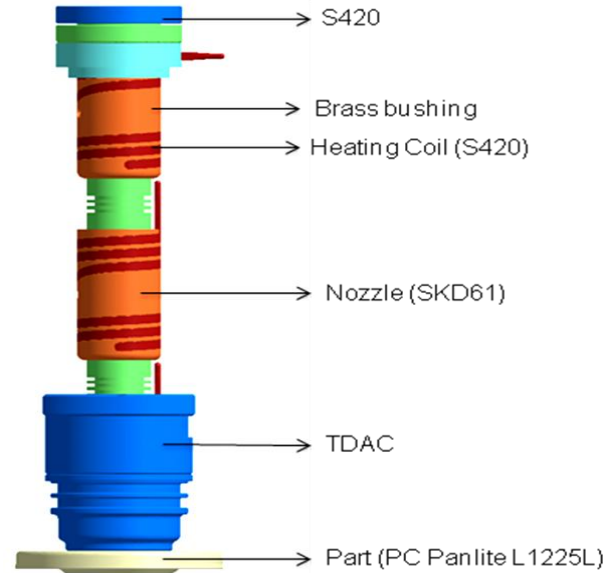


Fig. 1 The CAE model for hot runner system

Table 1 Material property for hot runner components

Material Properties for Hot Runner Components					
	P20 (Moldbase)	SKD61	Brass	TDAC	S420
Density (g/cm ³)	7.75	7.81	8.50	7.81	7.72
Heat Capacity (e+006 erg/g.K)	4.62	4.60	3.85	4.62	4.62
Thermal Conductivity (e+006 erg/sec.cm.k)	2.90	2.47	16	2.60	2.43

Table 1 lists the material properties, including density, heat capacity and thermal conductivity, for each hot runner components in this system. These parameters are the inputs in the analysis. This is to consider the effects from different thermal properties.

The figure 2 shows the information of boundary conditions and sensor node locations which is defined according to the real experiments. The surfaces highlighted in dark green color are defined as the contact areas with the metal mold. The undefined surfaces are automatically assumed as heat insulation due to air layer around these areas. The air is assumed as very poor heat conduction material. The number 1 to 10 sensor nodes are used to measure melt temperature function of time. These nodes are placed along the central line of hot runner nozzle. The number 11 to 17 sensor nodes (or 1A, 2A, 3A, 1B, 2B, 3B, 1C) are used to control on/off for the heating coils. For example, the sensor nodes 12, 13, and 14 (or 1A, 2A, 3A) are assigned to each heating coils respectively. The target temperature is 280°C and the range is ±2°C. The power for each heating coil is 400W or 610W as indicated in figure 3. If the sensor node 1A reaches the temperature of 282°C, the corresponding heating coil is switched off. On the contrary, if the temperature goes down to 278°C, the heating coil is turned on. This is the same for the sensor nodes 2A, 2B and their corresponded heating coils.

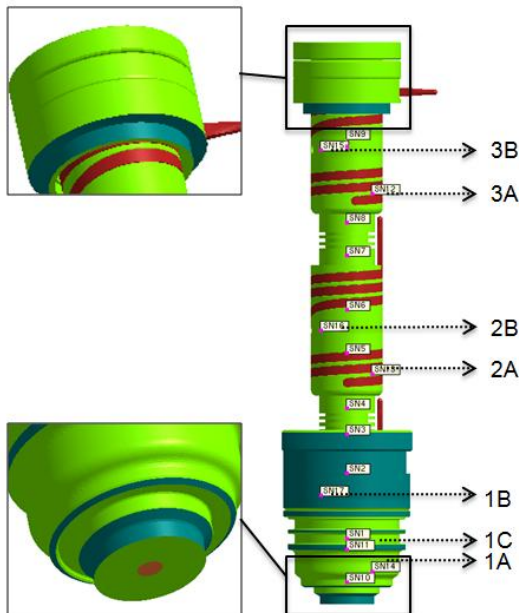


Fig. 2 Boundary conditions and sensor node positions

The filling time and packing time are both 5 seconds. The cooling channel layout and coolant (water) temperature is also shown in figure 3. The cooling time and open time is 20s and 5s respectively. They are

referred from the process condition in the real injection molding experiments. They are counted in one injection molding cycle for transient cool analysis. Therefore, the cycle time is 35 seconds. The melt temperature on the sensor nodes 1 to 10 can be predicted and compared with the experimental measurements.

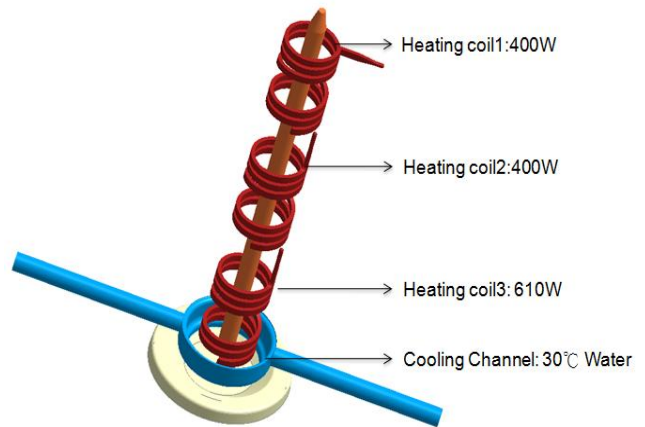


Fig. 3 Heating coils and cooling channel

Experimental Study

In the hot runner experiment, the injection molding process is conducted cycle by cycle. The melt temperature is measured at the same locations as the positions of sensor nodes 1 to 10 in the simulation. There are seven sensor lines arranged in the hot runner system which are represented by the sensor nodes (1A, 2A, 3A, 1B, 2B, 3B, 1C) in the simulation. The figure 3 shows hot runner system used in the experiment. The heating coils are connected to the power supplier. The figure 4 shows the metal mold in the experiment. The size of the moldbase is 250.00 x 250.00 x 320.00 mm. The figure 5 shows sensor lines embedded in the grooves of the hot runner nozzle. Each line is 0.2mm in diameter. The lines are connected to the power monitor for control of the heating coils. Table 2 shows the molding parameters. The temperature measuring will be applied after ten shots to make sure the melt temperature is stable.



Fig. 4 The hot runner system in the experiment

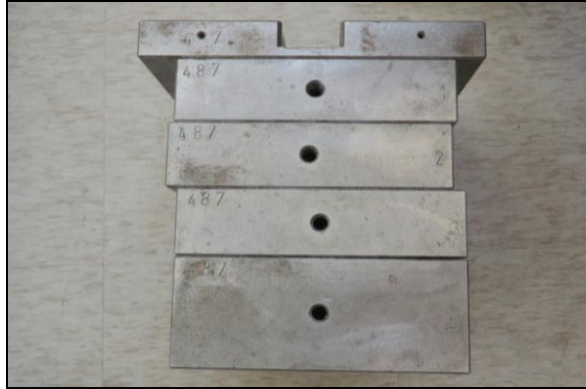


Fig. 5 Experimental metal mold



Fig. 6 Temperature sensor lines in the hot runner system

Table 2 Injection molding process parameters

Injection molding process condition	
Filling speed (mm/s)	40
Injection time (s)	5
Melt temperature (°C)	280
Mold temperature (°C)	80
Packing pressure (MPa)	10
Packing time (s)	5
Cooling time (s)	20
Mold open time (s)	5
Cycle time (s)	35

Results and Discussions

The simulating results are shown and discussed first, including melt temperature distribution inside of the melt channel and moldbase. The dynamic temperature history curves obtained from the sensor nodes are also displayed and investigated. In the experimental result, the melt temperature as function of the certain locations is measured and plotted. The simulating result is compared with that from the experiment. The comparison shows the good agreement both in trend and magnitude. This is to validate this simulation technology used for hot runner system.

The Simulation Results

The figure 7 displays the simulating melt temperature field inside the runner or melt channel at the end of ten injection molding cycles. The sensor node 2 detects higher melt temperature in the runner due to higher power from the heating coil around that area. The sensor node 10 detects much lower melt temperature because of the cooling channel and heat conduction contact with the metal mold in the hot runner system. The melt temperature field at different timing can be shown and observed also.

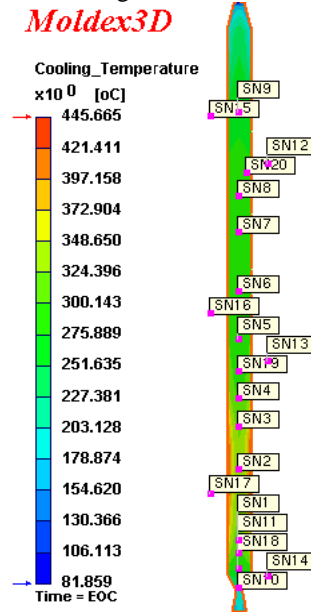


Fig. 7 Temperature profile in the runner after ten injection molding cycles

The figure 8 demonstrates the simulating temperature field inside of the moldbase after ten injection molding cycles. The moldbase near the cooling water has lower temperature as indicated in dark blue color.

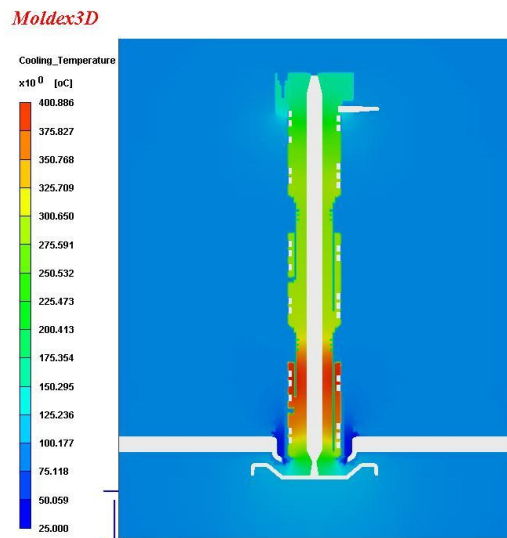


Fig. 8 Temperature profile inside of moldbase after ten injection molding cycles

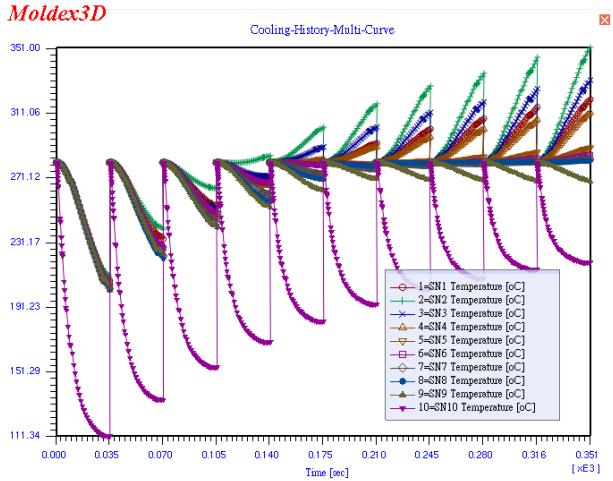


Fig. 9 Melt temperature history curves for the sensor nodes 1 to 10.

The figure 9 displays the simulating melt temperature history curves for the sensor nodes 1 to 10. This records the dynamic response of melt temperature cycle by cycle and allows for melt temperature investigation at the end of the specific cycle by extracting the data. It can be observed that the melt temperature on detected from each sensor node goes up cycle after cycle. Ultimately, the temperature should reach steady state after a long time. In this case, the temperature variation is smaller than 0.5% after ten molding cycles or 350 seconds. That means the melt temperature is nearly stable after many injection molding cycles.

The Validation from the Experiment

The figure 10 shows the experimental melt temperature distributions as function of location using controlling sensor nodes 1A, 2A, and 3A. The position zero means the location of the gate. The temperature was measured after several injection molding cycles and assumed to reach steady state. The simulating result is also plotted together and compared with the experimental one.

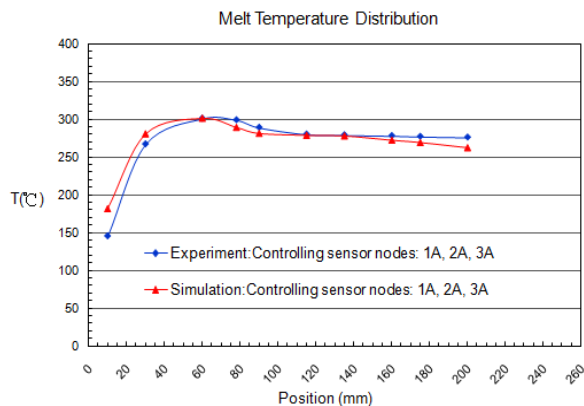


Fig. 10 Melt temperature distribution function of location for 1A, 2A, and 3A controlling sensor nodes

The figure 11 shows the experimental melt temperature distributions as function of location using controlling sensor nodes 1C, 2A, and 3A. Both the experimental and simulation results are similar to the case of controlling sensor nodes 1A, 2A, and 3A.

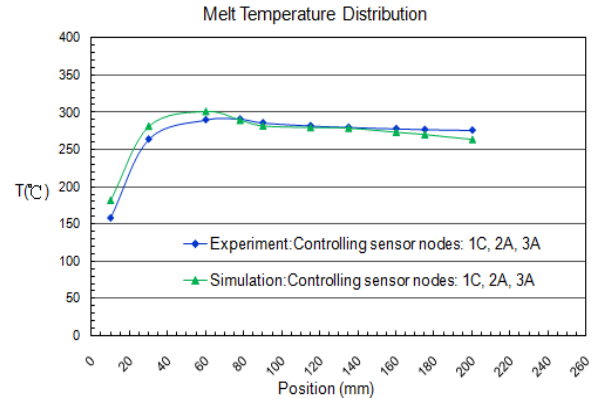


Fig. 11 Melt temperature distribution function of location for 1C, 2A, and 3A controlling sensor nodes

The figure 12 shows the experimental melt temperature distributions as function of location using controlling sensor nodes 1B, 2B, and 3B. In the experiment result, there is not obvious higher temperature region at the position of 60mm. The simulation result also indicates this phenomenon. This is different with the previous two cases.

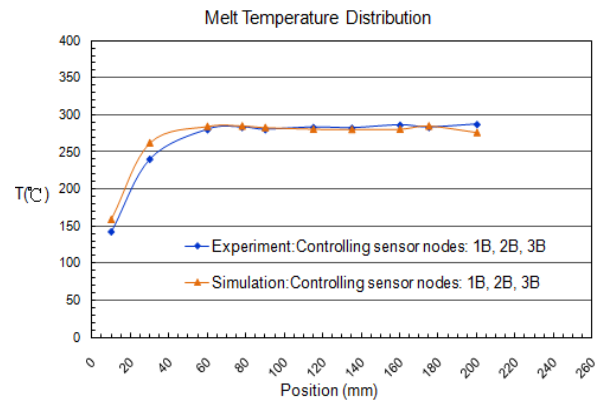


Fig. 12 Melt temperature distribution function of location for 1B, 2B, and 3B controlling sensor nodes

In the above three cases with different sets of controlling sensor nodes, the comparisons between the simulating and experimental results indicate good agreement in both trend and magnitude.

Conclusions

In this research, a true 3D numerical method to predict the temperature behavior in the hot runner system has been developed. A hot runner system CAE model can

be constructed, attribute-defined, and meshed in an efficient way in the preprocessing step. Through this numerical technique, the dynamic feature of temperature field in hot runner systems can be simulated and investigated. A real case from ANNTONG hot runner systems was used for the simulation. The simulating melt temperature profile can be obtained. The experimental study for this hot runner system is conducted and the melt temperature is measured at the locations of interest. The numerical results are compared with those from the experiment to validate Moldex3D simulation technology applied in this work. The simulating results are in good agreement with those from the experimental in both trend and magnitude.

References

1. T. A. Osswald, L. Turng and P. J. Gramann, Injection Molding Handbook, 2nd Ed., Hanser Gardner Publications, 2007.
2. S. Y. Yang and L. Lien, Intern. Polymer Procession, XI, 2, p188, 1996.
3. S. Y. Yang and L. Lien, Advances in Polymer Technology, 15, 3, p205, 1996..
4. S. C. Chen, Y. C. Chen and H. S. Peng, Journal of Applied Polymer Science, 75, p1640, 2000.
5. D. O. Kazmer, R. Nagery, B. Fan, V. Kudchakar, S. Johnston, ANTEC Tech. Papers 2005, 536.
6. G. Balasubrahmanyam, David Kazmer, ANTEC Tech. Papers 2003, 387.
7. Kapoor, D., Multi Cavity Melt Control in Injection Molding, M. S. Thesis, Submitted to the University of Massachusetts, Amherst, December 1997.
8. D. Frenkler, H. Zawistowski, "Hot Runners in Injection Moulds", Rapra publishers, Shawbury 1998, p.267.
9. B. Fan, D. Kazmer, ANTEC Tech. Papers 2003, 622.
10. Peter Unger, "Hot Runner Technology", Hanser Gardener Publication, 2006.
11. S. C. Chen, Y. C. Chen and N. T. Cheng, Int. Comm. Heat Mass Transfer, 25, 7, p907, 1998.
12. C. H. Wu and Y. L. Su, Int. Comm. Heat Mass Transfer, 30, 2, p215, 2003.
13. W. B. Young, Applied Mathematical Modelling, 29, p955, 2005.
14. R. Y. Chang and W. H. Yang, Int. J. Numerical Methods Fluids, 37, p125, 2001.
15. F. P. Incropera and D. P. DeWitt, "Introduction to Heat Transfer", John Wiley & Sons Inc, 1996.

Key Words: Hot runner; nozzle; heating coils; transient cool; Poisson's equation